Excitation of the $2p\sigma_u$ state of H_2^+ as a function of the internuclear axis alignment

M. A. Mangan, R. M. Wood, and A. K. Edwards
Department of Physics and Astronomy, University of Georgia, Athens, Georgia 30602-2451

Q. Zheng
Department of Natural Sciences, Indian River Community College, Fort Pierce, Florida 34981-5599

(Received 1 June 1998)

H_2 is bombarded by 400-eV electrons. Electrons scattered 18° with an energy loss of 36 eV are detected in coincidence with 7.6-eV H^+ fragments from the $2p\sigma_u$ state of H_2^+. The collision time and dissociation time are very small compared to the rotation time of the molecule. Therefore, the H^+ fragments leave the collision region along the line of the internuclear axis at the time of the interaction with the projectile. Angular distribution measurements of the H^+ ions yield the relative cross section for excitation of the $2p\sigma_u$ state of H_2^+ as a function of orientation of the internuclear axis. The data show a cosine-squared distribution relative to the momentum transfer vector of the collision. Calculations predicting the angular distribution are performed using prolate spheroidal coordinates. [S1050-2947(99)04101-3]

PACS number(s): 34.80.Gs, 34.50.Gb, 34.10.+x

I. INTRODUCTION

Many of the dynamical properties of multielectron atoms and molecules, such as double excitations and autoionizing transitions, occur through the mutual electron-electron interactions of the system. These electron interactions are called correlation [1]. Fast collisions that produce multielectron transitions are a useful way of studying electron correlation. The fast projectile has little time to interact with more than a single electron and consequently electron-electron interactions are responsible for a large part of the excitation cross section. The two-electron process of ionization plus excitation of an atom or molecule is an example. One electron of the target receives an impulse from the projectile and then, through correlation, imparts energy to the other target electron. The two-electron system of H_2 provides a unique opportunity to study this special process. *All* final states of excited H_2^+ are dissociative. They dissociate to produce H^+ fragments with energies related to the dissociative state. It is this property that we exploit in order to study the dynamics of electron correlation in this simple system.

Some of the early $(e,2e)$ experiments [2,3] were done to study correlation in the ground state of H_2. The final state of H_2^+ was either the ground state or an excited state. Theoretical analyses [4,5] of the experimental results were based on highly correlated ground-state wave functions of the target H_2. Theory did not satisfactorily match the results for the process of ionization plus excitation. Further experimental work [6] was done that covered a wider range of values of momentum transfer. More recent experimental and theoretical work [7] has been done that gives very good agreement with ionization without excitation but still fails for ionization with excitation.

Experiments have been started in our laboratory that measure relative cross sections for ionization and excitation processes in diatomic molecules caused by fast electrons, wherein the orientation of the internuclear axis is known to within a few degrees. The experimental procedure does not orient the molecules by applying a perturbation; it detects a fragment ion from those molecules that are dissociative and have axes aligned with a selected angle. The process is based on the axial recoil approximation (ARA) [8] and requires that the final state of the molecule be dissociative. The ARA states simply that for short collision times and rapid dissociation the molecule does not have time to rotate. Therefore, when a fast incident electron is scattered by a molecule with a fixed axis, the dissociation products travel along the line of this axis. Detection of one of the positively charged dissociation products by an angle- and energy-selective analyzer permits determination of the axis orientation and kinetic-energy release. Detection of a scattered electron of known energy loss or a decay product such as an Auger electron in a similar analyzer gives specific information about the final state of the reaction process. Scattering events of interest are signaled by the coincident detection of particles in the two analyzers. The procedure allows a variety of interactions and their properties to be studied as a function of the direction of the internuclear axis, which, until now, were lost due to the required integration over all angles of the molecular orientation.

It is no longer necessary to be as restrictive as the ARA. Computer codes have been developed that allow for inclusion of rotational motion, thermal translation, and instrumental broadening of the measured angular distributions [9].

This work studies orientational effects in the excitation of the $2p\sigma_u$ state of H_2^+ by fast electrons when the momentum transfer vector (and energy loss) are known. This state is formed by ionization plus excitation, i.e., by a two-electron process where electron correlation plays an important role. The relative cross section for the excitation of the $2p\sigma_u$ state as a function of the orientation of the internuclear axis relative to a known momentum transfer vector is measured and analyzed.

Previous measurements were made by us without a coincidence requirement. The purpose was to determine the dipole and nondipole contributions to the two-electron excitation and/or ionization of H_2 (double ionization, double excitation, and ionization plus excitation) by equivelocity

 ©1999 The American Physical Society

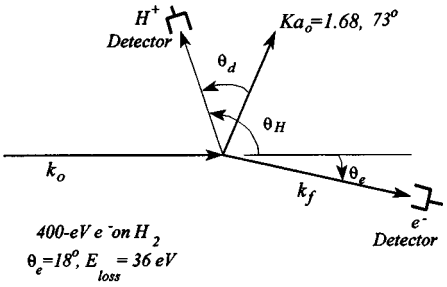

FIG. 1. Schematic diagram of the collision region. 400-eV electrons scattered 18° with an energy loss of 36 eV are detected in coincidence with 7.6-eV H^+ fragments. The H^+ detector is moved in angle and detects fragments from molecules aligned with it.

electrons and protons [10]. Calculations by Reading and Ford [11] had succeeded in predicting the differences in the double ionization of helium by positive and negative projectiles of equivelocity. They were able to show that this difference was due to the interference of dipole and nondipole contributions to the collision. Our early experiment was an attempt to show which two-electron processes in H_2 were strongly excited by dipole interactions with fast projectiles and which had a large nondipole part. These measurements, however, were not selective in momentum transfer or energy loss and included all possibilities.

More recent experiments studied the angular distribution of Auger electrons of N_2 in the molecular frame. Measurements [12–15] were made of the angular distribution in the molecular frame of the strongest Auger transitions in N_2. As a part of these studies coincidence measurements between Auger electrons and energetic N^+ fragments were made. To perform the analysis of the data, procedures for calculating wave functions and transition moments for homonuclear diatomic molecules in prolate spheroidal coordinates were developed [13,15].

II. EXPERIMENTAL PROCEDURE

A fast electron beam passes through an interaction region and is captured in a Faraday cup. The electron gun is set to produce a 400-eV electron beam. A collimator located 1.8 cm in front of the collision region is 0.8 mm in diameter. The H_2 target gas is in a differentially pumped region at room temperature. Needles or gas jets are not used, so that the H_2 does not have a nonisotropic velocity distribution that would disturb our angular measurements. At room temperature the most probable rotational level is $J=1$. During dissociation of the $2p\sigma_u$ state the molecular axis rotates about 2.5°.

Two identical hemispherical electrostatic analyzers are used: one to measure the energy and angle of the positive fragments ejected by the dissociating molecular ions and the other to detect the scattered electrons. The two analyzers are coplanar, one on each side of the electron beam, and each can be changed in angle independently of the other. In order for a H^+ fragment to be detected, the internuclear axis of the ionized H_2 must lie in the scattering plane and be aligned with the H^+ analyzer. A schematic of the experimental arrangement is shown in Fig. 1. The angular resolution of the analyzers is about $\pm 3\times 10^{-2}$ rad. The energy resolution of the analyzers is about 2% of the analyzing energy. Both analyzers are equipped with electrostatic zoom lenses that allow for acceleration or deceleration of the particles prior to energy analysis. The electron energy is reduced by a factor of 0.2 before analysis and the H^+ ions are increased in energy by a factor of 1.3.

The electron analyzer is placed at $\theta_e=18°$ with voltages set to pass electrons that have undergone an energy loss of 36 eV. For 400-eV electrons scattered at 18° with an energy loss of 36 eV, the momentum transfer vector is $\vec{K}a_0=1.67$ at 73°. The electron analyzer is set at 18° as a matter of convenience because of the geometry of the collision region. The minimum angle accessible is 15°. However, the combination of 400-eV incident energy and 18° scattering angle with 36-eV energy loss is a favorable condition for making the measurements of interest. They are the conditions to be near the top of the Bethe ridge [16] for excitation of the $2p\sigma_u$ H_2^+ state.

The voltages of the H^+ analyzer are fixed to analyze 7.6-eV H^+ ions (or 15.2-eV dissociation energy). The combination of measuring energy loss and dissociation energy allows one to select the $2p\sigma_u$ state. Energy loss determines which potential-energy curves of H_2^+ are energetically accessible in the Franck-Condon region via the collision. Dissociation energy determines the point on the curve at which the H^+ fragment is formed. For example, energy losses of about 33–43 eV and a dissociation energy of 15.2 eV (7.6 eV per particle) isolates the $2p\sigma_u$ state from the H_2^+ states that dissociate into $H^+ + H(nl)$ with $n \geq 2$.

Standard procedures are used to collect data. The signal from the detection of an electron starts a time-to-amplitude converter (TAC) and the signal from the fragment-ion analyzer stops the TAC. The output of the TAC goes to an analog-to-digital converter whose output is stored in a multichannel analyzer. A peak in the spectrum indicates time-correlated events. Because of the fine energy and angular resolution that are used, these measurements are very time consuming. The real coincidence count rate is about one per hour and data collection continues 24 h a day with breaks to record data and reset angles. Each data point in Fig. 3 is for an accumulated running time of about 10 days. The number of real coincident events recorded is divided by the number of scattered electrons detected. This divides out any effects in the measurements due to small changes in the beam current or target-gas pressure from run to run.

As the H^+ analyzer is moved in angle it becomes necessary to correct the data for the variation in the viewable target volume common to both detector systems and to correct for the change in the angular acceptance from each point in the common volume. The procedure for doing this is described in Ref. [9]. The positioning of the H^+ analyzer is limited in the forward direction by the presence of the electron detector at 18° and in the backward direction by the electron gun.

III. THEORY

In order to take advantage of the symmetry of homonuclear diatomic molecules we have selected to approach the problem using prolate spheroidal coordinates. The ''radial'' coordinates is $\xi_i=(r_{ia}+r_{ib})/d$ and the ''angular'' coordinates are $\eta_i=(r_{ia}-r_{ib})/d$ and φ_i, where d is the internu-

clear separation of the two protons, $r_{ia(b)}$ is the distance of the ith electron from proton a or b, and φ_i is the azimuthal angle measured around the internuclear axis (the z axis).

It is known [17] that an interaction potential of the form $[g(\xi)+f(\eta)]/(\xi^2-\eta^2)$ allows the Schrödinger equation to be treated by separation of variables. The Coulomb interaction of the H_2 system is of this form. This leads to a wave function $\psi(c;\xi,\eta,\varphi)=R_{mn}(c;\xi)S_{mn}(c;\eta)\Phi(\varphi)$, where $c^2=Ed^2/2$ and E is the energy. The functions $\Phi(\varphi)$, $S_{mn}(c;\eta)$, and $R_{mn}(c;\xi)$ are solutions of the differential equations

$$\frac{d^2}{d\varphi^2}\Phi(\varphi)+m^2\Phi(\varphi)=0, \tag{1}$$

$$\frac{d}{d\eta}\left[(1-\eta^2)\frac{d}{d\eta}S_{mn}(c;\eta)\right]+\left(A_{mn}-c^2\eta^2-\frac{m^2}{1-\eta^2}\right)S_{mn}(c;\eta)=0, \tag{2}$$

and

$$\frac{d}{d\xi}\left[(\xi^2-1)\frac{d}{d\xi}R_{mn}(c;\xi)\right]-\left(A_{mn}-c^2\xi^2-2\,dZ_{\text{eff}}\xi+\frac{m^2}{\xi^2-1}\right)R_{mn}(c;\xi)=0. \tag{3}$$

The φ equation has the usual solution, viz., $e^{im\varphi}$ with eigenvalue m. The coordinate $\eta=\cos\theta$, where θ is the angle of the asymptote of the hyperboloid of revolution of constant η. The spheroidal functions

$$Y_{mn}(c;\eta,\varphi)=S_{mn}(c;\eta)\frac{e^{im\varphi}}{\sqrt{2\pi}}$$

manifest the symmetry of the problem, much the same way as spherical harmonics in the atomic case. $S_{mn}(c;\eta)$ is even or odd depending on the reflection symmetry through a plane perpendicular to the internuclear axis at its center. The number of nodes in $S_{mn}(c;\eta)$ is given by the difference $n-m$. The quantum number m gives the number of nodal planes that contain the internuclear axis. The inversion symmetry is gerade if n is even and ungerade if n is odd. The symmetry operations of the point group $D_{\infty h}$ can be applied to the function $Y_{mn}(c;\eta,\varphi)$ and transformation properties established. These symmetry properties allow the molecular states and interactions investigated here to be discussed in terms of σ_g, σ_u, π_g, π_u, etc., symmetries just as atomic cases of spherical symmetry are discussed in terms of s, p, d, etc., states and waves. There is a difference however. The shape (but not the symmetry) of the function $Y_{mn}(c;\eta,\varphi)$ is dependent on the energy and internuclear separation d. In the united-atom limit where $d\to 0$, the functions $Y_{mn}(c;\eta,\varphi)$ reduce to the spherical harmonics $Y_{lm}(\theta,\varphi)$ if $S_{mn}(c;\varphi)$ is properly normalized [18].

Bound-state wave functions are generated by numerically integrating the Schrödinger equation. The conditions for starting the integration are determined by the Frobenius method. Symmetry arguments and known solutions of the united-atom limit are used to determine the number of nodes of the wave functions. For H_2, experimental values of the bound-state energy and internuclear separation d are used to calculate c. The separation constant A_{mn} is found by numerically integrating the η equation [Eq. (2)]. A_{mn} is inserted into the ξ equation [Eq. (3)] with the value of c. The ξ equation is integrated and the value of the charge of the nuclei Z_{eff} is adjusted to find the appropriate $R_{mn}(c;\xi)$. In order to generate H_2^+ wave functions (the one-electron problem), Z of each proton is set equal to 1 and the ξ and η equations are solved simultaneously for A_{mn} and c. The results are compared to the potential-energy curves of Sharp [19].

A partial-wave expansion in spheroidal functions [20] is used for the wave functions of the free electron ejected from H_2 in the ionization processes. The functions $S_{mn}(c;\eta)$ are found in terms of a series expansion [21] in associated Legendre functions. The recursion relation formed by this technique is used to find the separation constant. It is assumed that the outgoing wave represents an electron in the potential of the two nuclei screened by the remaining electron, which may be in the ground state or an excited state for the processes of interest. Numerical integration of the ξ equation with δ-function normalization and the proper boundary condition for large ξ yields the Coulomb phase shifts [22].

Many-body perturbation theory is used to calculate the transition moments. The processes included in the calculations are known in the literature as two-step 1 (TS-1) and shake-off and are shown in the Goldstone diagrams of Figs. 2(a) and 2(b) [1]. Time evolves from the bottom of the diagram to the top and arrows backward in time represent holes. In the first process [diagram 2(a)], the incident electron ejects a ground-state electron into a continuum intermediate state. The ejected electron interacts with the remaining bound electron and excites it to the $2p\sigma_u$ state. In the shake-off process [diagram 2(b)] the incident electron excites one electron to the $2p\sigma_u$ state and the other electron is ejected by an electron-hole interaction. Figure 2(c) shows shake-up, where the first electron is ejected and the second relaxes to the $2p\sigma_u$ state, but this process is not allowed by symmetry. The electron-hole interaction has σ_g symmetry and cannot excite the $1s\sigma_g$ electron to the $2p\sigma_u$ state. Figure 2(d) illustrates ground-state correlation, which was not included in our calculations.

The matrix elements to be calculated for Fig. 2(a) (TS-1) are of the form [1]

$$\frac{\langle 2p\sigma_u k'\lambda_f|v|1s\sigma_g k\lambda_i\rangle\left\langle k\lambda_i\left|\frac{4\pi}{K^2}e^{i\vec{K}\cdot\vec{r}}\right|1s\sigma_g\right\rangle}{E_0+\epsilon_{1s\sigma_g}-\frac{k_i^2}{2}-E_f+i\gamma}, \tag{4}$$

where $\vec{K}=\vec{k}_0-\vec{k}_f$ is the momentum transfer in the collision, E_0 and E_f are the energies of the fast electron before and after the collision, respectively, $\epsilon_{1s\sigma g}$ is the $1s\sigma_g$ bound-state energy, and k_i is the momentum of the ejected electron in the intermediate state. The subscripts i and f denote the intermediate and final states, respectively. The interaction v represents the electron-electron or electron-hole interaction r_{12}^{-1}. An expansion of r_{12}^{-1} in prolate spheroidal coordinates is used [23]. The matrix element on the right in the numera-

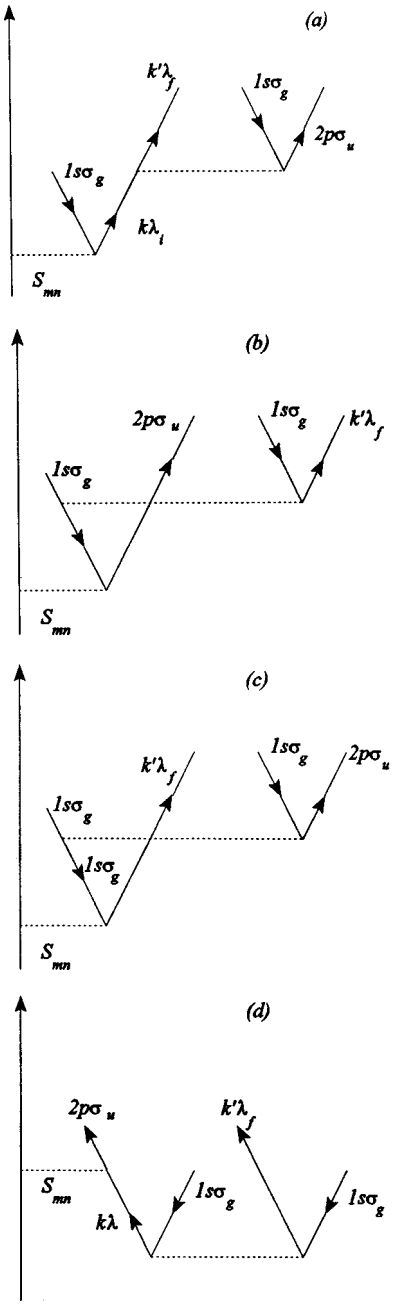

FIG. 2. Goldstone diagrams for the ionization plus excitation of H_2 to the $2p\sigma_u$ state of H_2^+: (a) TS-1, (b) shake-off, (c) shake-up (forbidden), and (d) ground-state correlation.

tor of Eq. (4) is due to the collision interaction and the other matrix element is from the correlation interaction.

The matrix elements for the shake-off process [1] depicted in Fig. 2(b) are

$$\frac{\langle k'\lambda_f 1s\sigma_g|\nu|1s\sigma_g 1s\sigma_g\rangle\left\langle 2p\sigma_u\left|\frac{4\pi}{K^2}\,e^{i\vec{K}\cdot\vec{r}}\right|1s\sigma_g\right\rangle}{E_0+\epsilon_{1s\sigma_g}-\epsilon_{2p\sigma_u}-E_f}, \quad (5)$$

where $\epsilon_{2p\sigma u}$ is the $2p\sigma_u$ bound-state energy. Exchange terms are included as well as sums and integrals over intermediate and final states as needed.

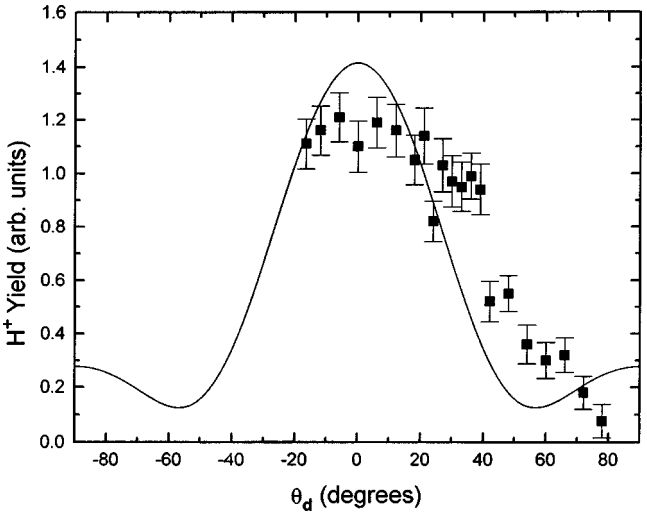

FIG. 3. Ionization plus excitation of the $2p\sigma_u$ state of H_2^+ as a function of the angle between the internuclear axis and the momentum transfer vector. The smooth line is a one-parameter fit of the calculated values to the data. Error bars signify statistical errors.

The factor $e^{i\vec{K}\cdot\vec{r}}$ in the collision matrix element is expanded in partial waves [20] and contains the function $S_{mn}(c;\cos(\theta_d))$, where θ_d is the angle between $\vec{K}$ and the internuclear axis $\vec{d}$. It is this term that contains the angular dependence that is being measured. Included in these calculations are $m=0$ and $n=0,2$ (σ_g symmetry), $m=0$ and $n=1,3$ (σ_u symmetry), and $m=1$ and $n=1$ (π_u symmetry) for the collision interaction. Each of the partial waves in the collision interaction expansion determines the symmetry of the intermediate state that appears in the correlation matrix element. All possible symmetries of the intermediate states from the listing above are included. All possible symmetries of the continuum final states from the listing above are included with the addition of $m=1$ and $n=2$ (π_g symmetry). It is the product of the collision term with the subsequent correlation matrix element that determines the relative contribution of each partial wave to the cross section. Only the energy conserving term is included in the TS-1 calculation. Integration over the intermediate-state momenta is done. The coherent sum of all amplitudes is multiplied by its complex conjugate and integrated over the momenta of the outgoing wave of the final state. The calculated values are fit to the measurements by only one parameter.

IV. RESULTS AND DISCUSSION

The measured angular distribution and the calculated values are shown in Fig. 3. The error bars on the data points are statistical only. Based on the calculations presented here, the TS-1 process dominates shake-off. The smooth curve in Fig. 3 shows no discernible difference with and without the inclusion of the shake-off process. This is not unexpected. Shake-off is more probable when the initial interaction quickly removes an electron from the target rather than simply exciting it [24].

The largest contributor to the calculated cross section is an electron-molecule interaction of σ_g symmetry with $n=2$, i.e., $S_{02}(c;\cos(\theta_d))$, that leads to an intermediate state of

like symmetry. This interaction term is primarily d wave, $m=0$, in the molecule's frame. The final state for this interaction is the excited H_2^+ and a continuum electron of σ_u symmetry [$Y_{01}(c;\eta,\varphi)$, primarily p wave, $m=0$]. Both the collision matrix element and the correlation matrix element are larger for this case than for the next largest contributing combination. The next largest term is the σ_u interaction $S_{01}(c;\cos(\theta_d))$ leading to a σ_u intermediate state and a σ_g continuum state $Y_{00}(c;\eta,\varphi)$ for the ejected electron. In the calculated intensity the $S_{01}(c;\cos(\theta_d))$ contribution is about 28% the value of the largest component. The d-wave nature of the leading term of the calculation can be seen in the smooth curve fit to the data. It peaks when the internuclear axis is aligned with the momentum transfer vector and has minima near $\pm 54°$, i.e., the transition moment has a large $P_{20}(\cos(\theta_d))$ component. The data itself is fit best by a cosine-squared distribution in the intensity, meaning a σ_u interaction, $S_{01}(c;\cos(\theta_d))$, in the transition moment.

In our earlier work [10] the scattered electron was not detected and only the H^+ fragment ions were detected. The momentum transfer vector was unknown and all fragments as a function of kinetic energy (dissociation energy) as well as orientation of the internuclear axis were observed. Calculated kinetic-energy spectra of H^+ fragments for several states were fit to the measured spectra to ascertain the respective contributions of each dissociative state to the total spectrum. That work resulted in a cosine-squared distribution for the $2p\sigma_u$ excitation where the axis of quantization was in the laboratory frame and perpendicular to the beam axis. It was argued that a dipole interaction would produce such an angular distribution.

The analysis of the data has omitted two commonly considered interactions [1]. These are ground-state correlation and double collisions (TS-2). It may be that one or both of these might enhance the S_{01} contribution of the transition moment and yield a better fit between theory and experiment. However, calculations by Parikh [25] have shown that at 400-eV collision energy TS-1 should be much greater than TS-2. On the other hand, El Mkhanter and Dal Cappello [26] have shown that it is necessary to include TS-2 in the double ionization of helium even at high collision energies for certain $(e,3e)$ experiments.

ACKNOWLEDGMENTS

The authors thank M. M. Duncan for his many helpful discussions and continued interest in the experiment. We also thank Jim Feagin for a most helpful visit to our laboratory. This work was supported by the National Science Foundation under Grant No. PHY-9307129.

[1] J. H. McGuire, *Electron Correlation Dynamics in Atomic Collisions* (Cambridge University Press, Cambridge, 1997).
[2] E. Weigold, S. T. Hood, I. E. McCarthy, and P. J. O. Teubner, Phys. Lett. **44A**, 531 (1973).
[3] E. Weigold, I. E. McCarthy, A. J. Dixon, and S. Dey, Chem. Phys. Lett. **47**, 209 (1977).
[4] J. W. Liu and V. H. Smith, Phys. Rev. A **31**, 3003 (1985); **39**, 3703 (1989).
[5] J. W. Liu, Phys. Rev. A **32**, 3784 (1985); **38**, 1659 (1988).
[6] M. Chérid, A. Lahmam-Bennani, A. Duguet, R. W. Zurales, R. R. Lucchese, M. C. Dal Cappello, and C. Dal Cappello, J. Phys. B **22**, 3483 (1989).
[7] N. Lermer, B. R. Todd, N. M. Cann, Y. Zheng, C. E. Brion, Z. Yang, and E. R. Davidson, Phys. Rev. A **56**, 1393 (1997).
[8] R. N. Zare, J. Chem. Phys. **47**, 204 (1967).
[9] R. M. Wood and A. K. Edwards, in *Accelerator-Based Atomic Physics Techniques and Applications*, edited by S. M. Shafroth and J. C. Austin (AIP, New York, 1997); R. M. Wood, Q. Zheng, A. K. Edwards, and M. A. Mangan, Rev. Sci. Instrum. **68**, 1382 (1997).
[10] A. K. Edwards, R. M. Wood, M. A. Mangan, and R. L. Ezell, Phys. Rev. A **46**, 6970 (1992).
[11] J. F. Reading and A. L. Ford, J. Phys. B **20**, 3747 (1987).
[12] Q. Zheng, A. K. Edwards, R. M. Wood, and M. A. Mangan, Phys. Rev. A **52**, 3940 (1995).
[13] Q. Zheng, A. K. Edwards, R. M. Wood, and M. A. Mangan, Phys. Rev. A **52**, 3945 (1995).
[14] A. K. Edwards, Q. Zheng, R. M. Wood, and M. A. Mangan, Phys. Rev. A **55**, 4269 (1997).
[15] Q. Zheng, Ph.D. dissertation, University of Georgia, 1995 (unpublished).
[16] M. Inokuti, Rev. Mod. Phys. **43**, 297 (1971).
[17] M. Aubert, N. Bessis, and G. Bessis, Phys. Rev. A **10**, 51 (1974); **10**, 61 (1974).
[18] L. I. Ponomarev and L. N. Somov, J. Comput. Phys. **20**, 183 (1976).
[19] T. E. Sharp, At. Data **2**, 119 (1971).
[20] C. Flammer, *Spheroidal Wave Functions* (Stanford University Press, Stanford, 1957).
[21] J. A. Stratton, P. M. Morse, L. J. Chu, J. D. C. Little, and F. J. Corbató, *Spheroidal Wave Functions* (Wiley, New York, 1956).
[22] H. Nakamura and H. Takagi, Nagoya University, Institute of Plasma Physics Report No. IPPJ-AM-16, 1980 (unpublished).
[23] K. Rüdenberg, J. Chem. Phys. **19**, 1459 (1951).
[24] J. H. McGuire, N. C. Deb, O. L. Weaver, T. Ishihara, L. Kocbach, and T. Mukoyama, Nucl. Instrum. Methods Phys. Res. B **40/41**, 340 (1989).
[25] M. Parikh, Phys. Rev. A **12**, 1872 (1975).
[26] R. El Mkhanter and C. Dal Cappello, J. Phys. B **31**, 301 (1998).